

Effects of nonstoichiometry in the melting process of Y_2O_3 from molecular dynamics simulations

Luis Javier Álvarez*

*Departamento de Física, Facultad de Ciencias, Universidad Autónoma del Estado de Morelos,
Avenida Universidad No. 1001, Chamilpa, Cuernavaca, Morelos, 62210, Mexico*

Miguel Angel San Miguel

Departamento de Química Física, Facultad de Química, E-41012, Sevilla, Spain

José Antonio Odriozola†

*Departamento de Química Inorgánica e Instituto de Ciencia de Materiales,
Universidad de Sevilla—Consejo Superior de Investigaciones Científicas, E-41012 Sevilla, Spain*

(Received 10 August 1998)

Molecular dynamics simulations in the microcanonical ensemble of liquid yttrium oxide were performed at a temperature of 3100 K. Three different Y/O ratios were used in order to find out what the role of nonstoichiometry is in the process of melting and disordering of the liquid at high temperatures. Our simulations indicate that when no oxygen vacancies are generated there is no disordering process and the crystalline structure should remain. We conclude that the melting process occurs, in the real system, when a large enough number of oxygen vacancies is generated as a result of the large thermal vibrations of superficial oxygen atoms. The apparent high coordination number for yttrium found experimentally is explained based on the overlapping of the partial radial distribution functions, which cannot be elucidated from the x-ray diffraction data but can be clearly seen from our simulations. [S0163-1829(99)08813-X]

I. INTRODUCTION

X-ray diffraction experiments at high temperatures have recently been performed to elucidate the structure of liquid aluminium and yttrium oxides, since the knowledge of structural properties of supercooled liquid yttrium-aluminum garnet (YAG) can be achieved by knowing the terminal phases Al_2O_3 , and Y_2O_3 .^{1,2} We reported recently the results of molecular-dynamics simulations which allowed us to refine the interpretation of the structure of liquid aluminum oxide from the x-ray-diffraction experiments reported in Ref. 1. Yttrium oxide has been described as substoichiometric at high temperature and low oxygen partial pressure.^{2,3} However, in the experiments reported in Ref. 2, the authors estimate that, because of the high oxygen contents of the ambient gas in which they perform their experiments, the sample could be considered stoichiometric, although they report a mass loss, upon melting, of nearly two percent. If the mass loss is due to the generation of oxygen vacancies in the material, instead of Y_2O_3 , we would have $Y_2O_{2.7175}$, which represents about 9.42% of oxygen species lost.

Computer simulation of materials has proved to be a very important resource to help understanding experimental data, especially in the case where extreme thermodynamic conditions are required.^{4,5} In the report of the experiments by Krishnan *et al.*² they interpret their results postulating that supercooling molten yttria causes a decrease in the first coordination shell and Q values together with an increase in the Y-O interionic distance. In the melt the average coordination number for yttrium, according to their interpretation, goes to 7.5, far beyond 6 which is the coordination number in crystalline yttria.

In computer simulations it is a natural result to have the

partial as well as total radial distribution functions, and therefore, an easy task to estimate coordination numbers and interionic distances. This allows us to assess the hypotheses based on x-ray experimental data, to analyze the effect of nonstoichiometry on the melting process, and to resolve the conflict posed by the different results on the melting temperature of yttrium oxide. In this paper we present the results of three different molecular dynamics simulations of the yttrium oxide systems with three different stoichiometries and show what the role of stoichiometry is in the melting process.

II. SIMULATION PROCEDURE

In order to explore the role of stoichiometry in the melting process we performed three simulations with ratios O/Y equal to 1.5, 1.458, and 1.375 corresponding to Y_2O_{3-x} , where $x=0$, $x=0.083$, and $x=0.25$, respectively. The simulations were performed in the microcanonical ensemble with a system consisting of 2160, 2124, and 2052 particles, respectively, of which 864 represented yttrium atoms and the rest oxygen atoms arranged in a cubic box. To obtain the “samples” with less oxygen contents, oxygen atoms were removed at random from the crystalline, perfectly stoichiometric structure. The pair interaction potential is a Pauling-type function which has proven to be a fairly good way of representing the partially covalent interaction in metal oxides for molecular dynamics simulations,⁴⁻⁶ and is given by

$$V(r_{ij}) = \frac{q_i q_j}{r_{ij}} + \frac{1}{n(\sigma_i + \sigma_j)} \left(\frac{\sigma_i + \sigma_j}{r_{ij}} \right)^n,$$

TABLE I. Pair interaction potential parameters.

		Y_2O_3	$Y_2O_{2.917}$	$Y_2O_{2.75}$
Atom	$\sigma/\text{\AA}$		q/e	
Y	0.89	2.10	2.10	2.100 037 5
O	1.38	1.40	1.44	1.5273

where q_i are effective charges; σ_i are the effective atomic radii taken from Shannon and Prewitt⁷ and n was taken to be 9 as was proposed by Adams and McDonald⁸ for ionic systems. The values of these parameters are shown in Table I. The long-range Coulombic interactions were calculated using the Ewald summation method.⁹

The Pauling-type potential depends only on the atomic effective radii σ , and the effective charges q . In order to determine the charges of particles representing yttrium and oxygen atoms we chose to fit the heat of formation of Y_2O_3 reported to be -455.38 kcal/mol,¹⁰ which in the simulation is simply the total potential energy of the system. In order to test the ability of the interaction potential to reproduce the thermodynamic properties of yttria, we calculated the variation of the heat of formation ΔH^0 , as a function of temperature in the temperature range 2300–3200 K only for the stoichiometric system. Figure 1 shows the behavior of ΔH^0 vs T . The discontinuity of the straight line between 2700 and 2750 K shows that the melting occurs roughly around 2725 K, which is in extraordinary agreement with the experimental value estimated from spectral emissivity measurements of 2731 K.²

All three simulations started with a solid structure in a computational box with periodic boundary conditions, whose volume was set 10% higher than the normal to account for the volume expansion reported to occur upon melting.² The simulation schedules consisted of a run of 10 ps at 3100 K rescaling the velocities of all particles every time step. Then a run of 10 ps without temperature control in order to relax the system to assure the thermodynamic equilibrium; finally

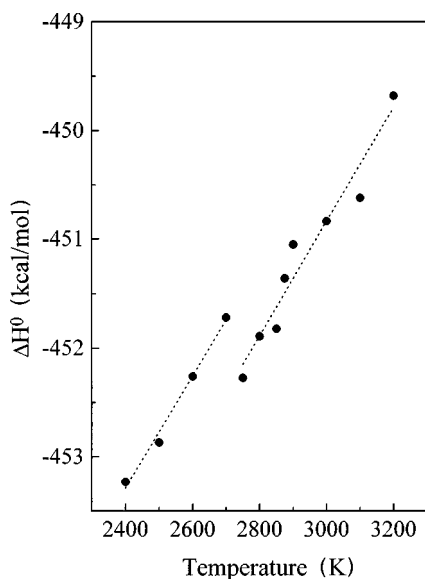


FIG. 1. Variation of the heat of formation ΔH^0 as a function of temperature in the temperature range 2300–3200 K.

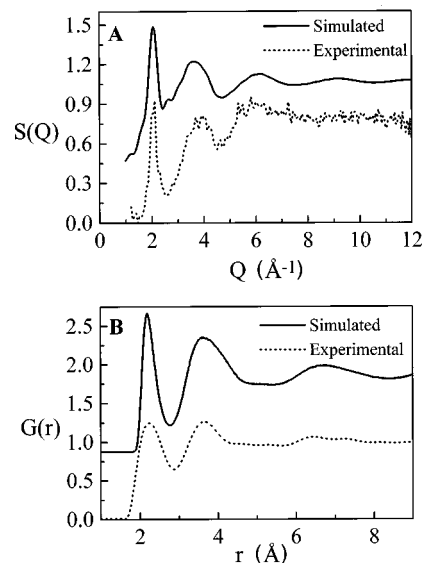


FIG. 2. Structure factor $S(Q)$ and total radial distribution function $G(r)$ for the experimental system and the $Y_2O_{2.75}$ simulated system.

a run of 5 ps in which accumulation of the relevant quantities was performed to calculate statistical averages. In this last run of the molecular dynamics program temperature fluctuations were of the order of plus or minus 14 K. The integration of the classical equations of motion was carried out using the leap-frog algorithm with an integration time step of 10^{-15} s. Energy fluctuations were of 0.01 kJ/mole around the mean value.

As it can be seen from Table I the effective charges of oxygen atoms were adjusted to preserve the electroneutrality of the nonstoichiometric systems. It seems reasonable to increase the effective charge of oxygen atoms since in the real system the loss of mass observed upon heating would imply the creation of oxygen vacancies. The resulting O_2 species leave behind electric charge which spreads over the whole system.

III. RESULTS AND DISCUSSION

Molecular dynamics simulations allow for the direct calculation of the partial radial distribution functions $g(r)$, as

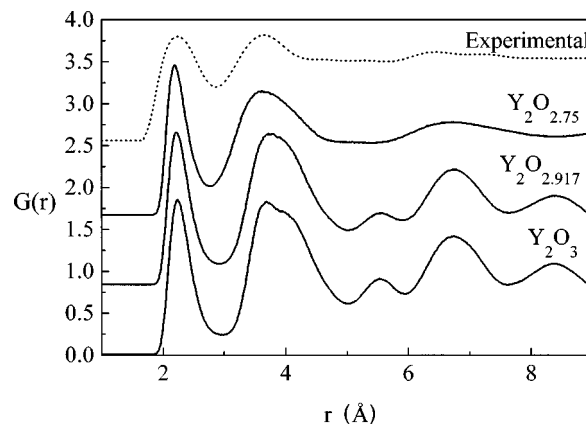


FIG. 3. Experimental and simulated $G(r)$ for the Y_2O_3 , $Y_2O_{2.917}$, and $Y_2O_{2.75}$ systems.

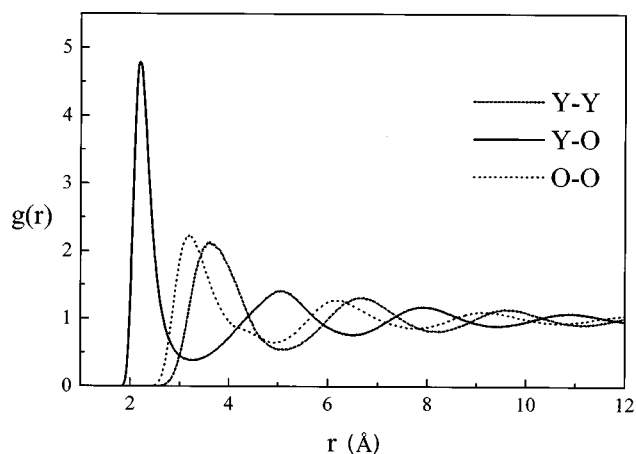


FIG. 4. Partial radial distribution functions $g(r_{YY})$, $g(r_{YO})$, and $g(r_{OO})$ for the $Y_2O_{2.75}$ simulated system at 3100 K.

well as the total radial distribution function $G(r)$ and the structure factor $S(Q)$, whose comparison with their experimental counterparts is straightforward. Figure 2 shows both the structure factor, and the total radial distribution function for the experimental and the $Y_2O_{2.75}$ simulated system. As it can be seen from the figure there is an excellent agreement for both $S(Q)$ and $G(r)$, between experimental data for the sample at the highest temperature reported of 3039 K in Ref. 2 and the calculated for the $Y_2O_{2.75}$ theoretical sample. Figure 3 shows the $G(r)$ for the theoretical samples of Y_2O_3 , and $Y_2O_{2.917}$ and $Y_2O_{2.75}$ along with the corresponding experimental one. The curve of the $Y_2O_{2.75}$ has only reminiscences of the original crystalline structure whereas the other two still have long-range order. The simulated $G(r)$ show that the vacancies of oxygen atoms are necessary for the system to lose the long-range order, and to really become a liquid, which agrees with the experimental fact that heating the system in an atmosphere poor in oxygen produces a significant decomposition and loss of mass.

Looking at the three $g(r)$ for the pairs Y-Y, Y-O, and O-O for this last simulation shown in Fig. 4 one can clearly notice the overlapping of the first peaks of the pairs Y-O and O-O, up to a distance of 3.39 Å, at which the minimum of the Y-O function occurs. The estimation of the coordination number for the pair Y-O by direct integration of the total radial distribution function may lead to different results depending on the distance up to which the integration is performed. On the other hand, as mentioned above, there is an

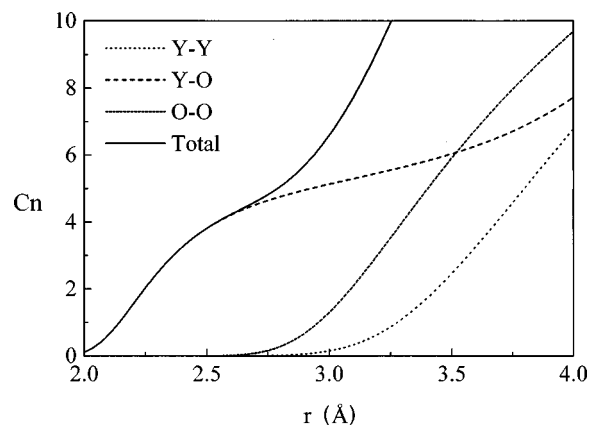


FIG. 5. Coordination number (Cn) calculated by integrating the partial radial distribution functions shown in Fig. 4.

important overlapping of the Y-O and O-O functions which becomes more important at high temperatures due to thermal vibrations. Therefore the coordination number of the pair Y-O is overestimated when it is done based on the experimental $G(r)$. Figure 5 shows the integrals under the partial radial distribution functions obtained from our simulation of the $Y_2O_{2.75}$ sample. The solid line is the sum of the three partial integrals. As it can be seen from the figure the rapid variation of the curve corresponding to the O-O pair is responsible for both the apparent high coordination number estimated experimentally of 7.5 ± 0.8 , and the large uncertainty with which it has been determined. From a careful coordination analysis of the resulting configuration from our simulations we obtained a distribution of coordinations with an average coordination number of 5.09 for the Y_4O pair. Table II shows a summary of coordination numbers for the pairs Y-O and O-O. The average coordination number of oxygen is 3.70 which is very close to 3.88 for the perfectly stoichiometric sample, which means that the Y_4O polyhedra are essentially preserved in the melt independently of the number of oxygen vacancies. This suggests that the structural model for C- Ln_2O_3 proposed by Caro,¹¹ which builds up the three-dimensional solid by the Ln_4O tetrahedra sharing four out of six edges, is valid for liquid yttria.

The effect of nonstoichiometry in both coordination numbers and bond distances can be understood by observing the positions of the maxima in the $G(r)$ plots shown in Fig. 3. As the Y/O ratio increases there is a shift to the left of the first two peaks which is what is observed in the high-

TABLE II. Summary of coordination numbers for the pairs Y-O and O-O for the three different stoichiometries.

Cn	Y-O			O-O		
	Y_2O_3	$Y_2O_{2.917}$	$Y_2O_{2.75}$	Y_2O_3	$Y_2O_{2.917}$	$Y_2O_{2.75}$
2				4	9	20
3			7	145	212	410
4	4	31	172	1147	1036	662
5	146	313	434		3	95
6	713	516	237			1
7	1	4	14			
Total	864	864	864	1296	1260	1188

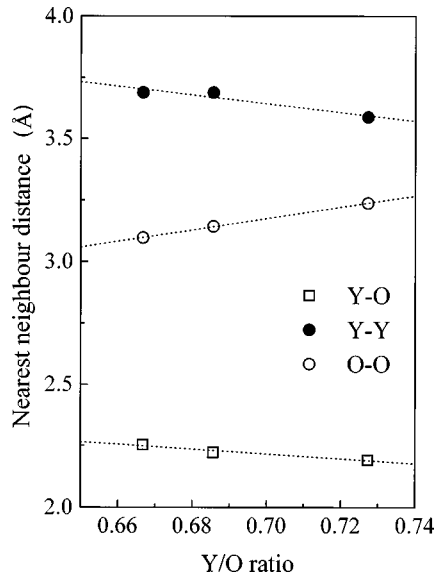


FIG. 6. Nearest-neighbor distances as a function of the Y/O ratio of the simulated systems. Y_2O_3 , $Y_2O_{2.917}$, and $Y_2O_{2.75}$.

temperature x-ray experiments of Ref. 2. To understand this effect we have plotted in Fig. 6 the nearest-neighbor distances for the three pairs Y-Y, Y-O, and O-O vs the Y/O ratio for the three simulations we have performed. As it can be seen two different behaviors are present. One, is to shorten the nearest-neighbor distance for the pair Y-Y and Y-O on increasing the Y/O ratio. On the other hand, the O-O corresponding distance increases as the Y/O decreases. What this all means is that the generation of oxygen vacancies strengthen the Y-O bond due to the decrease of steric repulsion between oxygen atoms. Therefore, both Y-Y and Y-O distances decrease. Since there is a smaller number of oxygen atoms when the Y/O ratio increases, the average O-O distance increases.

A 500 K variation in temperature should promote changes in the Y/O ratio of the solid, increasing the number of oxygen vacancies when the temperature is increased. It is worth noticing that the loss of mass in the x-ray experiments we have been referring to, is estimated at the end of the experimental schedule, therefore the real situation of the material at high temperatures remains unknown. From the linear relationships shown in Fig. 6, and the experimental data on the positions of the first and second peaks of $G(r)$, we have estimated the Y/O equivalent ratios. A summary of these estimations is shown in Fig. 7. This shows that in the real system the stoichiometry is not preserved. Assuming a linear relationship between Y/O ratio and temperature in the whole temperature range this loss of stoichiometry would start at temperatures as low as 1500 K. If our estimations are correct in the real experiments there is a loss of oxygen atoms which amounts up to 15% at high temperatures.

In our simulations there is a clear dependency of the order-disorder relationship on the Y/O ratio, which is evidenced in the shape of the radial distribution functions $G(r)$, in which there are maxima and minima very well defined up to 9 Å for the systems Y_2O_3 and $Y_2O_{2.917}$ (see Fig. 3). Experimentally the estimated formula for the yttrium oxide would be $Y_2O_{2.67}$ at the melting point. The mobility of anions can be increased at lower temperatures if the Y/O ratio

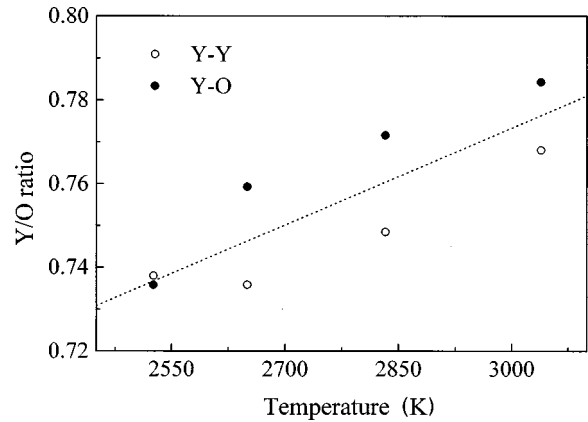


FIG. 7. Estimated Y/O ratios as a function of temperature for the distances to the first and second peaks of the experimental $G(r)$.

decreases which, according to the experimental evidence and our present considerations, is equivalent to lowering the oxygen fugacity.

Our simulations along with the experimental procedure followed and reported by Krishnan and co-workers, strongly suggest that this effect must be general, and should apply to other oxides and certainly would be the case of the yttrium-aluminum garnet. This opens a way to process materials in the YAG system by modifying oxygen fugacity and temperature.

IV. CONCLUSIONS

We have performed molecular dynamics simulations of yttrium oxide with three different Y/O ratios in order to find out what the role of nonstoichiometry is in the process of melting and disordering of the liquid at high temperatures, well above the melting point. This was suggested by the experimental evidence that there is a loss of mass upon melting of the material when it is done in an atmosphere poor in oxygen. Our simulations indicate that when no oxygen vacancies are generated there is no disordering process and the crystalline structure should be preserved. We conclude that the melting process occurs, in the real system, when a large enough number of oxygen vacancies is generated as a result of the large thermal vibrations of superficial oxygen atoms. This is in agreement with what has been observed in the high-temperature experiments, where there is a partial pressure of O_2 . From our simulations the apparent high coordination number for yttrium is explained based on the overlapping of the partial radial distribution functions, which cannot be elucidated from the x-ray diffraction data.

ACKNOWLEDGMENTS

This work was partially supported by the Comisión Interministerial de Ciencia y Tecnología (MAT97-0717), Spain. The x-ray diffraction data were kindly supplied by Dr. Shankar Krishnan from Containerless Research, Inc., Evanston Illinois, L.J.A. thanks Consejo Nacional de Ciencia y Tecnología (CONACYT), México for financial support for sabbatical leave.

- *On sabbatical leave from Laboratorio de Simulación de Materiales, DGSCA, Universidad Nacional Autónoma de México, México D.F., Mexico.
- †Author to whom correspondence should be addressed. Electronic address: odrio@cica.es
- ¹S. Ansell, S. Krishnan, J. K. R. Weber, J. J. Felten, P. C. Nordine, M. A. Beno, D. L. Price, and M. L. Saboungi, *Phys. Rev. Lett.* **78**, 464 (1997).
- ²S. Krishnan, S. Ansell, and D. L. Price, *J. Am. Ceram. Soc.* **81**, 1967 (1998).
- ³R. J. Ackerman and R. J. Thorn, *Science of Ceramics*, edited by G. H. Stewart (Academic, New York, 1961), p. 397.
- ⁴M. A. San Miguel, J. Fernández Sanz, L. J. Alvarez, and J. A. Odriozola, *Phys. Rev. B* **58**, 2353 (1998).
- ⁵M. A. San Miguel, L. J. Alvarez, J. Fernández Sanz, and J. A. Odriozola, *Phys. Rev. B* **58**, 6057 (1998).
- ⁶L. J. Alvarez, L. E. León, J. Fernández Sanz, M. J. Capitán, and J. A. Odriozola, *Phys. Rev. B* **50**, 2561 (1994); *J. Phys. Chem.* **99**, 17 872 (1995); J. P. Jacobs, M. A. San Miguel, L. J. Alvarez, and P. Bosch Giral, *J. Nucl. Mater.* **232**, 131 (1996); P. Jacobs, M. A. San Miguel, J. E. Sánchez Sánchez, and L. J. Alvarez, *Surf. Sci.* **389**, L1147 (1997).
- ⁷R. D. Shannon and C. T. Prewitt, *Acta Crystallogr., Sect. B: Struct. Crystallogr. Cryst. Chem.* **25**, 925 (1969).
- ⁸D. J. Adams and I. R. McDonald, *Physica B* **79**, 159 (1970).
- ⁹P. P. Ewald, *Ann. Phys. (Leipzig)* **64**, 253 (1921).
- ¹⁰*CRC Handbook of Chemistry and Physics*, 63rd ed., edited by R. C. Weast and M. J. Astle (CRC Press, Boca Raton, FL, 1982).
- ¹¹P. E. Caro, *J. Less-Common Met.* **16**, 367 (1968).